

Impact-acoustics-based health monitoring of tile-wall bonding integrity using principal component analysis

F. Tong^a, S.K. Tso^{b,*}, M.Y.Y. Hung^b

^a*Key Laboratory of Underwater Acoustic Communication and Marine Information Technology of the Ministry of Education, Xiamen University, Xiamen, China*

^b*Consortium for Intelligent Design, Automation and Mechatronics, Department of Manufacturing Engineering and Engineering Management, City University of Hong Kong, Hong Kong SAR, China*

Received 31 August 2005; received in revised form 14 November 2005; accepted 19 November 2005

Available online 24 January 2006

Abstract

The use of the acoustic features extracted from the impact sounds for bonding integrity assessment has been extensively investigated. Nonetheless, considering the practical implementation of tile-wall non-destructive evaluation (NDE), the traditional defects classification method based directly on frequency-domain features has been of limited application because of the overlapping feature patterns corresponding to different classes whenever there is physical surface irregularity. The purpose of this paper is to explore the clustering and classification ability of principal component analysis (PCA) as applied to the impact-acoustics signature in tile-wall inspection with a view to mitigating the adverse influence of surface non-uniformity. A clustering analysis with signature acquired on sample slabs shows that impact-acoustics signatures of different bonding quality and different surface roughness are well separated into different clusters when using the first two principal components obtained. By adopting as inputs the feature vectors extracted with PCA applied, a multilayer back-propagation artificial neural network (ANN) classifier is developed for automatic health monitoring and defects classification of tile-walls. The inspection results obtained experimentally on the prepared sample slabs are presented and discussed, confirming the utility of the proposed method, particularly in dealing with tile surface irregularity. © 2006 Elsevier Ltd. All rights reserved.

1. Introduction

For the purpose of external decoration and wall protection, bonded tile-walls are widely employed on the high-rise buildings in big cities like Hong Kong. However, due to improper installation, climate effects or aging, there is an increasing number of tile dropping accidents caused by adhesive failure or bonding defect [1–2]. Because these bonding defects can hardly be detected by naked eyes, an effective non-destructive inspection method is necessary to avoid the hazards posed.

For bonding integrity inspection inside layered structures [3–6], various non-destructive evaluation (NDE) methods have been extensively developed. However, in the application of integrity assessment over external walls of high-rise buildings, the adoption of classic strategies such as ultrasound-echo and impact-echo is

*Corresponding author. Tel.: +852 2788 8061; fax: +852 2788 8423.

E-mail addresses: ftong@xmu.edu.cn (F. Tong), meskts@cityu.edu.hk (S.K. Tso).

hindered by the need to maintain a good contact between the sensor and target specimen, which is difficult or inconvenient to be realized at heights or on large tested areas. Meanwhile, other non-contact techniques such as holography, X-rays or laser are too environment-sensitive and generally too expensive.

Considered to be a cost-effective approach where it is not necessary to glue the sensor with the tested object, the impact sounds method is the subject of investigation for tile-wall bonding assessment in this paper. As an established inspection method, the methodology of impact acoustics strategy is based on the fact that if two bonded materials are impacted with a small, hard object, the characteristics of sounds emanated will vary depending on the bond quality. The operation of this method is simple and cheap, but is unfortunately subjective and operator dependent.

To remove its dependence on the human ear and experience, there have appeared many efforts to automate the impact test operation [7–9]. In most of the previous investigation, the assessments are conducted based on direct use of the impact sounds' spectra distribution. Asano [8] derived from the frequency distribution impact acoustics parameters for developing a defects detection system. In another frequency-distribution-based investigation [9], Wu defined the ratio of the power of the lower 1/3 frequency range to that of the overall frequency range in the impact-sounds spectrum as the *power accumulation ratio factor* and used it to characterize the integrity of multilayered materials.

Unfortunately, the features directly obtained from the corresponding portions of signature spectra are found to be sensitive to the surface irregularities of the target surface, as the interaction between the impactor and the target surface in a nominally single tap would lead to overlapping patterns between different bonding integrity. As a result, under physical environments where surface non-uniformity is unavoidable, the actual assessment performance of the impact-acoustics method based on the direct frequency-domain will be seriously affected.

Principal component analysis (PCA) is a useful statistical signal processing technique to reduce the dimensionality of data sets for compression, pattern recognition and data interpretation [10,11]. In the present work, it is applied as an unsupervised clustering method for acoustic signatures generated in impact NDE test. The input vector to the clustering procedure is selected to be the normalized power spectral density (PSD) of the signatures. PCA is then performed for dimension reduction and feature extraction of the impact-acoustics data. Through clustering analysis of the signatures obtained on artificial slabs, satisfactory clustering ability as well as good immunity to the surface roughness of target is observed. Thus, a novel NDE method based on incorporating PCA and a multilayer artificial neural network (ANN) is developed for high-reliability tile-wall inspection. Experimental classification results are finally presented, demonstrating the effectiveness of the proposed method for practical tile conditions.

2. Theoretical basis of PCA

As a widely used statistical technique, PCA has, in practice, been employed to reduce the dimensionality of problems, and to transform interdependent coordinates into significant and independent ones. Because PCA has been well documented in multivariate analysis literature [10], its concept is only briefly introduced in this section.

The main basis of PCA-based dimension reduction is that PCA picks up the dimensions with the largest variances. Mathematically, this is equivalent to finding the best low rank approximation (in L2 norm) of the data via the angular value decomposition [11]. Essentially, by rotating the data such that maximum variabilities are projected onto orthogonal axes, a set of correlated variables are transformed into a set of uncorrelated variables which are ordered by reducing variability. The uncorrelated variables are linear combinations of the original variables, and the last of these variables can be removed with minimum loss of real data [12].

Consider that there exists n objects and each object has k variables, and these objects can be composed into an $(n \times k)$ -dimensional data matrix, X . In this investigation, each object is an experimentally obtained impact-acoustics data with k points. These n objects can be plotted in a k -dimensional variable space and objects (data sets) having similar appearance would be grouped close to each other and form a subspace. However, when the number of dimensions is large, this k -dimensional space is abstract and impossible to visualize. PCA is a multivariate procedure which fits an approximate model to represent the data matrix X with a reduced number

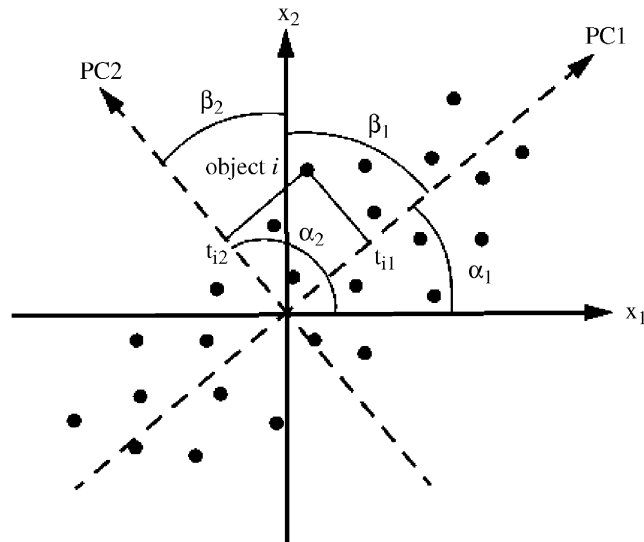


Fig. 1. Illustration of principal components analysis (PCA).

of relevant dimensions by rotating the data such that maximum variabilities are projected onto the axes. Essentially, a set of correlated variables are transformed into a set of uncorrelated variables which are ordered by reducing variability. The uncorrelated variables are linear combinations of the original variables, and the last of these variables can be removed with minimum loss of real data.

In Fig. 1, two principal components (PC1 and PC2) have been identified after the PCA. PC1 matches the maximum variance and PC2 is orthogonal to the first PC and it accounts as much as possible for the remaining variance. This procedure can mathematically be expressed as a split of the original data into a sum of a matrix product, TP^T , and a residual matrix E ,

$$X = TP^T + E, \tag{1}$$

where T is the so-called score matrix and its columns consist of the score vector, t_i , associated with the principal components, PC_i . The score vector contains each object's score value for a corresponding principal component, i.e. each object's coordinate in a direction of maximum variance, which is found as described earlier. The loading matrix P has each variable's loading vector, p_i , in its columns. Each value in the loading vector is the cosine of the angle between the considered principal component and the original variable. Therefore, these loading vectors express how much a certain principal component has in common with each variable. Acting as an indicator of how close this model is to the original data, the residual matrix, E , contains the part of the original data set, X , which has not been accounted for in TP^T .

In the PCA of the earlier considered $(n \times k)$ -dimensional data matrix X , each score vector t_i and each loading vector p_i consists of n and k components, respectively. Assume N as the chosen number of the principal components, Eq. (1) may be decomposed as

$$X = t_1p_1^T + t_2p_2^T + \dots + t_Np_N^T + E. \tag{2}$$

Thus, the PCA provides a useful tool to show the inherent structure of the original data with reducing variability, which may be used to visually explore subgroups formed by objects exhibiting similar appearance.

3. Theoretical basis of impact acoustics

To relate the characteristics of an impact acoustic signature with the corresponding bonding state, impact dynamics analysis has been extensively conducted in the literature. For simplicity, the healthy and delaminated bonded target structures are modeled as isotropic thick rigid plate and flexible thin plate, respectively, with different thickness h (see Fig. 2(a) and (b)).

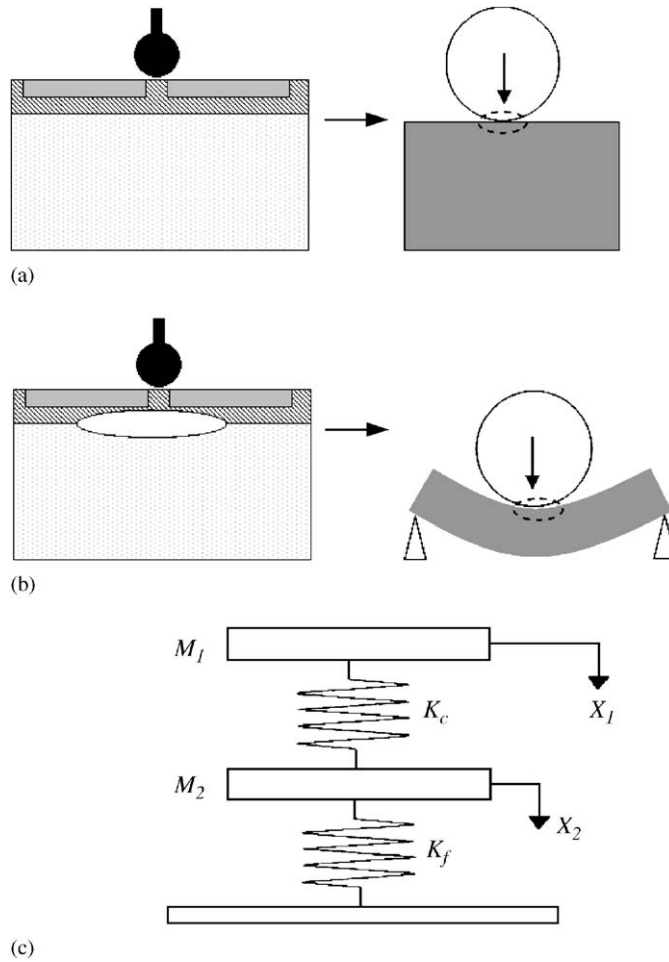


Fig. 2. Modeling of impact system.

A two-degree-of-freedom spring–mass model is used for consideration (see Fig. 2(c)) [13–15], consisting of one spring with K_f representing the bending stiffness of the tile-wall, another spring with K_c representing the nonlinear contact stiffness, and two bodies with M_2 and M_1 representing the effective mass of the delaminated tiled wall region and of the impacting sphere, respectively. Considering the impact between the two masses, the dynamics equations of the system can be written as

$$M_1 \frac{d^2 x_1}{dt^2} + P = 0, \quad (3)$$

$$M_2 \frac{d^2 x_2}{dt^2} + K_f x_2 - P = 0. \quad (4)$$

The contact of impacting bodies is of considerable interest in the comprehension of the impact response. Timoshenko [14] adapted Hertz's contact law in the impact of elastic spherical bodies, i.e.

$$P = K_c \alpha^{3/2}, \quad (5)$$

$$\alpha = x_1 - x_2, \quad (6)$$

where P is the contact force which is a nonlinear function of the indentation α , which is the difference between the motion of the two bodies along the vertical axis, in Fig. 2(c).

Considering the energy distribution in the impact process, assuming that the structure behaves quasi-statically, when the structure reaches its maximum deformation, the velocity of the sphere becomes zero and all of the initial kinetic energy will be converted to the energy stored by the deformation of the structure.

Therefore, ignoring the shear and membrane components of structure deformation, the energy balance equation can be given as

$$E_{\text{sum}} = \frac{1}{2} M_1 v_0^2 \approx E_f + E_c = E_f + E_{c1} + E_{c2}, \tag{7}$$

where v_0 is the initial velocity of the sphere, the subscript sum represents the overall energy of two bodies; the subscripts f, c refer to the energy stored in the structure’s bending deformation and contact region’s indentation (c_1 for sphere, and c_2 for tested structure), respectively.

Defining *vibration energy loss factor* λ as the ratio of energy transformed into flexural free-vibration of the target during the impact to the overall energy, according to Ref. [16], the following expression can be obtained:

$$\lambda = \frac{E_f}{E_{\text{sum}}} = \frac{1}{16} \left(\frac{M_2 K_c}{\rho h K_f} \right)^{1/2}, \tag{8}$$

where h, ρ are the thickness and density of the plate, respectively, and

$$K_c = \frac{4}{3} ER^{1/2}, \tag{9}$$

$$K_f = \frac{4\pi h^3}{3a^2} \left(\frac{E_2}{1 - \nu_2^2} \right), \tag{10}$$

where parameters R and E are defined as

$$\frac{1}{R} = \frac{1}{R_1} + \frac{1}{R_2}; \quad \frac{1}{E} = \frac{1 - \nu_1^2}{E_1} + \frac{1 - \nu_2^2}{E_2},$$

herein R_1 and R_2 are the radii of curvature of the two impacting bodies (for the case of the impact between sphere and plate, R_1 is the radius of the spherical impactor, $1/R_2 \approx 0$). The Young’s modulus and Poisson’s ratios of the two bodies are E_1, ν_1 and E_2, ν_2 , respectively.

Let $k_{12} = (1 - \nu_1^2/E_1)/(1 - \nu_2^2/E_2)$ and consider $M_2 = \rho h \pi a^2$; λ can be obtained as

$$\lambda \approx \frac{1}{16} \frac{R_1^{1/4}}{\sqrt{1 + k_{12}}} \frac{a^2}{h\sqrt{h}}. \tag{11}$$

Because k_{12} and R_1 are fixed parameters here, Eq. (11) suggests that the percentage of energy converted into flexural vibration is dependent on the thickness and radius of the circular plate. Based on acoustics theory, the intensity of sound radiation is proportional to the vibration energy. Thus, the intensity of sound excited by flexural vibration after the impact can be used as an indicator for the structure-integrity identification of the tile-wall.

Accordingly, for a degraded bonding structure, modeled as thin flexible plate, which has much less thickness and size than that of the healthy structure, most of the kinetic energy of the impactor will be converted to the flexural mode free-vibration. Conversely, the loss of kinetic energy of the sphere is very small when impacting on a rigid thick plate. Thus, the relative intensities of sound radiation excited by ringing of the sphere and plate can indicate the bonding integrity of the tile-wall structure.

Owing to the fact that the time components of ringing of impactor and tiled wall in impact sounds overlap and are difficult to be separated in the time domain, generally it is convenient to convert the signal into frequency domain with FFT algorithm for further examination. Therefore, most previous research of impact-acoustics NDE relied on the features directly extracted from the PSD for detection and classification purpose.

4. Experimental setup

In order to investigate the practical characteristics of the impact-acoustics signature, experiments are carried out on artificial sample slabs. To simulate the physical bonding status, 3 types of sample slabs are prepared.

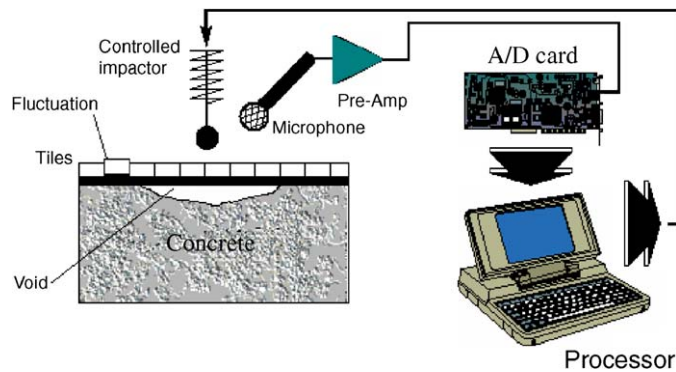


Fig. 3. Experimental setup.

One is a tiled-concrete slab of good bonding strength (called solid 1 class); the second type of tiled-slab contains a $\varnothing 140$ mm circle-shaped void at concrete substrate layer at the center location.

When considering the simplified impact mode, the influence of the target surface roughness on the resulting acoustic signature is ignored. However, it is observed that the abnormal multiple contacting behaviors caused by the surface irregularity greatly affect the actual acoustic characteristics. So the third type of samples slab is specially prepared to feature good bonding integrity and rough surface formed by edges of tiles (called solid 2 class). The dimensions of all the slabs are: 400 mm \times 400 mm \times 150 mm.

The NDT experimental system is illustrated in Fig. 3. The apparatus adopted includes: a rigid steel sphere of diameter 12 mm pushed by a coil used as the controlled impactor; a pre-amplifier module; an A/D converter card with 40 kHz sampling rate; a highly directional microphone. Such an impacting system generates a well-defined and simple input which in turn excites impact sounds with characteristics that facilitate signal interpretation.

5. Results

5.1. Signature obtained and analysis

In time-domain, each time history contains 1024 signal points sampled at 40 kHz, triggered by the pulse used to activate the impactor. To obtain the frequency-domain information, the PSD of the signature is obtained with the 1024-point fast Fourier transform (FFT) calculation based on the original time history. To remove the influence of impact strength, the resulting PSD is then normalized with its maximal magnitude to get the normalized PSD.

The typical signals obtained experimentally are illustrated in Figs. 4–6. From the resulting PSD curves, it is observed that the resonance peak of steel sphere's ringing, which is much stronger in solid slab than in debonded ones, is located within 8–10 kHz as shown in Fig. 4(b), while that of target structure's multiple mode flexural vibration lies in a lower range (see Fig. 5(b)). As shown in Figs. 4(b) and 5(b), the relative strength of these two components of impact sounds is in good agreement with previous theoretical assessment, considering their corresponding bonding status.

Furthermore, for solid structures, tapping on the rough surface of the solid 2 class slab leads to multiple interactions between impactor and the target surface in a nominally single tap [7]. Owing to the multiple contacts between the impactor and the surface of the solid target, the resulting time history shows different distribution from that of slab 1 (called solid 1 class), with multiple acceleration peaks and weak ringing component (see Fig. 6(a)). As a result, in the corresponding normalized PSD, the energy distribution exhibits fuzzy characteristics, including some overlapping pattern compared to that of slab 1 and debonded cases (see Fig. 6(b)) in the corresponding frequency ranges.

The experimental analysis above shows that, for the case of normal impact, the distribution of PSD curve can clearly indicate the existence of bonding defects and may produce a feasible indicator for inspection and

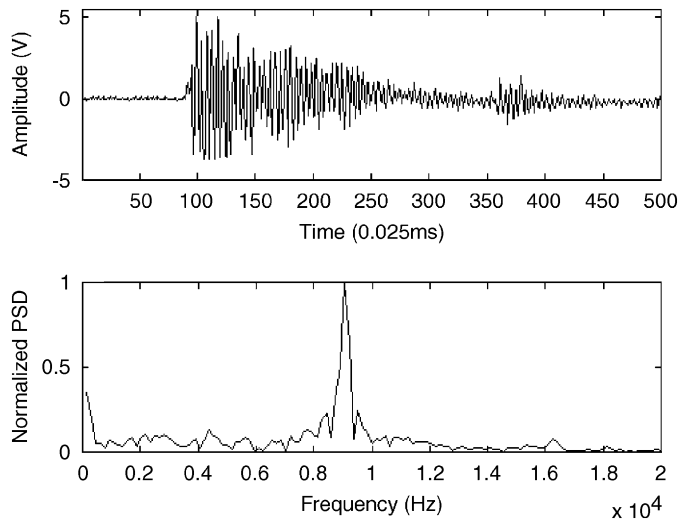


Fig. 4. Typical time history and normalized PSD of impact sounds from solid 1 slab.

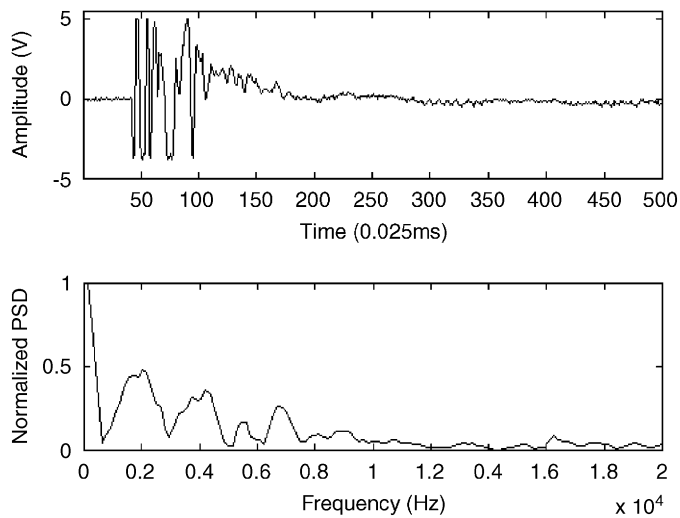


Fig. 5. Typical time history and normalized PSD of impact sounds from defective slab.

classification. However, the abnormal tap caused by surface irregularities will impose difficulty on the characterization of bonding property with the resulting overlapping pattern in PSD.

5.2. PCA implementation

In terms of developing an automatic defects assessment system, the presence of the solid 2 class lead to confusion between the major bonding types of signatures in normalized PSD, thus compromising the performance of the traditional PSD-based inspection method.

In this study, PCA is performed in order to explore its ability of variability reduction and clustering. The input data set X of PCA is the normalized PSD of the impact-acoustics signature. The number of observations is $n = 1200$, assembled from 400 solid 1, 400 solid 2 and 400 debonded class data. The length of each analyzed data set is $k = 256$, representing the first 256 points in the normalized PSD, i.e. covering the 0–10 kHz frequency band, which can reflect the main differences of the 3 classes.

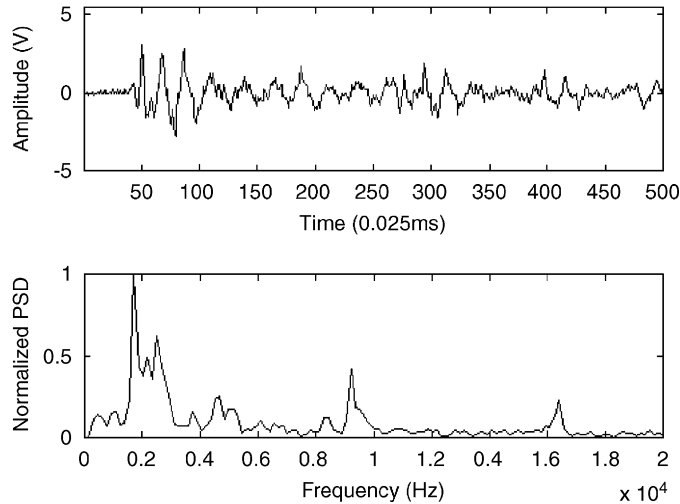


Fig. 6. Typical time history and normalized PSD of impact sounds from solid 2 slab.

In this work, the PCA is performed with the following eigenvector algorithm [17]:

- (1) calculation of the normalized covariance matrix C_X from the original PSD data matrix X ;
- (2) by eigenvector decomposition of the C_X , obtaining the eigenvectors U_i ($i = 1, 2, \dots, k$) and corresponding eigenvalues λ_i ($i = 1, 2, \dots, k$) sorted in descending order;
- (3) obtaining the principal components PC_i ($i = 1, 2, \dots, k$) by projecting the X onto the resulting eigenvectors U_i ;
- (4) to ensure sufficient accuracy, selecting the top N principal components PC_i ($i = 1, 2, \dots, N$) according to the associated eigenvalue λ_i ($i = 1, 2, \dots, N$), which is a measure of the amount of variance described by each PC_i .

Defining $R_N = \sum_{i=1}^N \lambda_i / \sum_{i=1}^K \lambda_i$ as the *accumulative contribution rate* of the top N principal components (where k is the total number of principal components), which indicates the percentage of the total variance in the observations explained by the top N principal components, the number N of the top principal components chosen as feature vector is determined accordingly. It is also straightforward to infer that a big R_N corresponds to a less significant residual matrix E . In this study, an R_N threshold of 0.6 leads to the number of principal components $N = 2$ for the observations tested, i.e., adopting only PC1 and PC2 for clustering test and feature extraction.

5.3. Clustering analysis

Meanwhile, for comparison, the vector with the same length ($N = 2$) is also chosen directly from the normalized PSD of the impact-acoustics signal. According to the impact dynamics study and experimental observation, the areas within the frequency range of 8–10 and 0–8 kHz, which contain the resonance information of the impactor and the multiple-mode flexible free-vibration of the defective structure, respectively, are defined as P1 and P2.

The clustering results of the PCA and PSD method are shown in Fig. 7(d) and (e), respectively, in their feature space. As seen in the score plot of PC1 and PC2 (see Fig. 7(d)), solid 1, solid 2 and debonded samples give rise to three well-separated clusters, which correspond to different bonding property and surface roughness in the slabs. However, in a P1 versus P2 score plot, (see in Fig. 7(e)), while solid 1 and debonded objects fall into clusters which can be discriminated from each other clearly, the solid 2 set exhibits fuzzy borders to the neighboring solid 1 and debonded classes, caused by the overlapping pattern mentioned earlier.

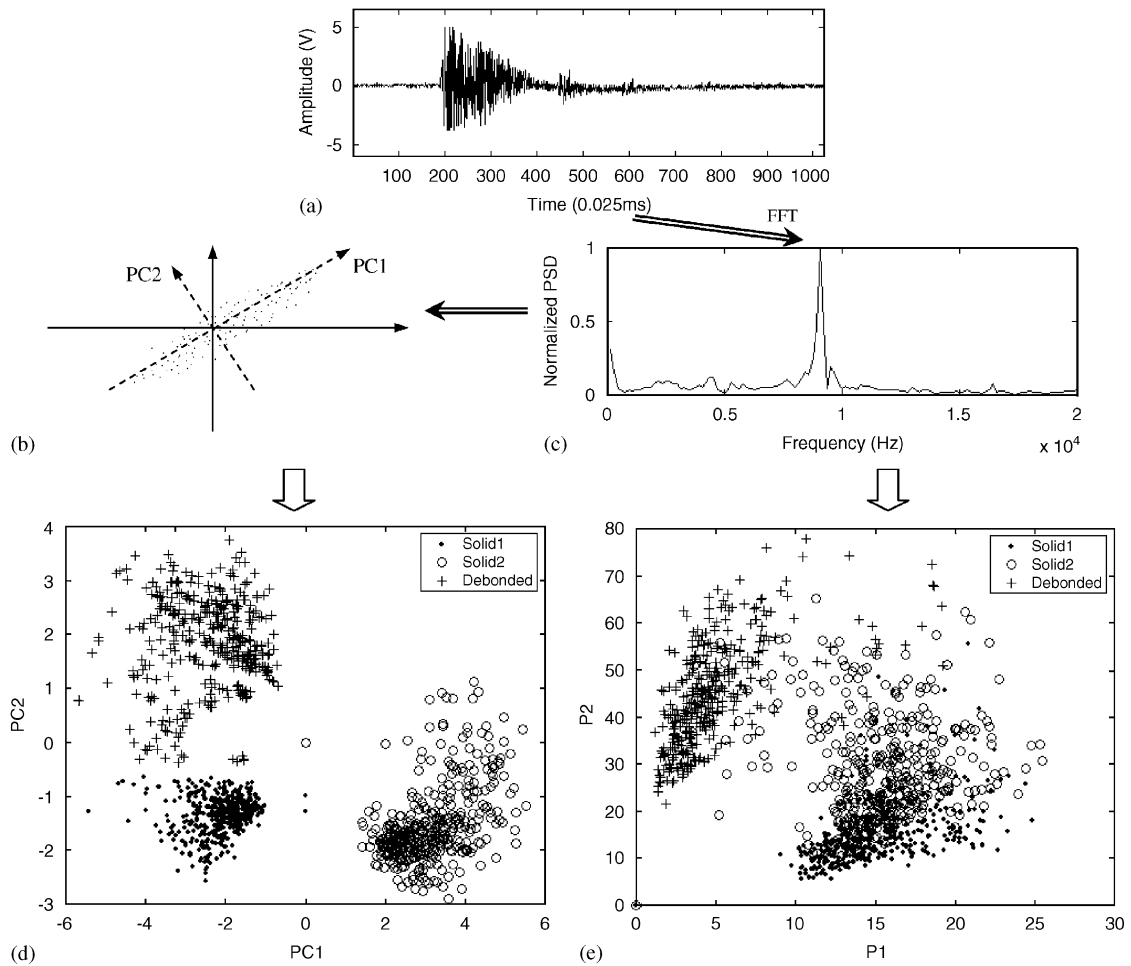


Fig. 7. Waveform (a) and normalized PSD (c) of acoustic signal, PCA processing (b), clustering results from the PCA (d) and direct normalized PSD (e) of sample slabs.

From the results of signatures clustering, it is seen that the PCA strategy would outperform the method using the original PSD data in terms of assessment of the bonding integrity property with the same dataset dimension.

6. Classification with neural network

6.1. ANN design

To facilitate the signal interpretation and automatic classification, a three-layer back-propagation neural network is employed as the classifier to perform the detection [18]. The ANN used consists of a 2-neuron input layer, one hidden layer and a 2-neuron output layer (see Fig. 8). The hidden layer has 8 neurons. The error back propagation (BP) method with a momentum updating algorithm is applied to train the ANN.

The ideal training output of the neural network is the binary bonding state of tile-wall, with (1, 0), (0, 1) and (0, 0) representing the solid 1, solid 2 and defective class, respectively. The raw outputs of the trained ANN will be determined based on the threshold (set to be 0.5 here) to obtain the final 0 or 1 binary output couple representing bonding results.

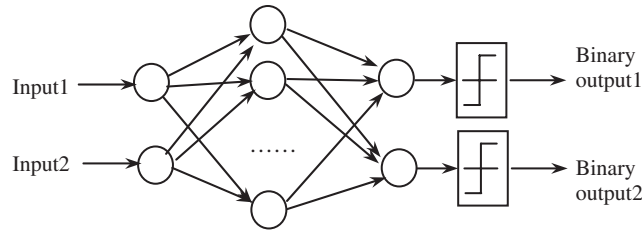


Fig. 8. Schematic diagram of ANN used.

Table 1
ANN output using PCA features

	Classification output			Accuracy rate (%)	Number of test cases
	Solid 1	Solid 2	Defect		
Solid 1	199	1	0	99.5	200
Solid 2	0	199	1	99.5	200
Defect	0	0	200	100	200

Table 2
ANN output using PSD features

	Classification output			Accuracy rate (%)	Number of test cases
	Solid 1	Solid 2	Defect		
Solid 1	179	21	0	89.5	200
Solid 2	12	182	6	91	200
Defect	4	0	196	98	200

The first two principle components, PC1 and PC2, obtained from PCA are used as the feature vector of the ANN. On the other hand, the parameters directly extracted from the normalized PSD, P1 and P2, are employed as the feature vector for comparison study.

6.2. Classification results

In this study, impact sounds obtained in the laboratory with 3 typical sample specimens mentioned above are divided into a training set and a test set. The training set of the sample data is used to train the network and the trained ANN is evaluated with the test set, exclusively. The training set contains 200 samples of solid 1, 200 samples of solid 2 and 200 samples of debonded signatures. The test set contains the same number of samples. In the training process, the training set is randomly selected to provide enough information for the learning algorithm.

The classification results of the ANN classifier are presented in Tables 1 and 2. In this study, the influence of the surface roughness is considered. With the use of feature vectors extracted by PCA, the accuracy rate of the solid 2 class is 99.5 for both solid classes and 100% for identifying the debonded case, confirming the good distinguishing ability of the PCA approach with respect to bonding property and surface roughness. On the contrary, the accuracy rate obtained with the raw normalized PSD feature vectors shows low sensitivity to the surface roughness of slabs, the accuracy rate being 89.5%, 91% for solid 1 and solid 2 classes, respectively.

Moreover, due to the overlapping effects in the feature space caused by surface irregularity, the detection rate of debonded class is 98%, which implies failure to detect 2% of the debonded cases.

7. Further discussion and conclusion

In this paper, the NDE method based on acoustic features obtained from impact sounds is investigated for bonding integrity inspection of the layered structure. However, most of the previous works made use of features extracted directly in the frequency domain, which are found to be less reliable whenever the target surface is rough. As a result, the practical implementation of impact test method for tile-wall inspection has not been widely applied to cases with large number of tile edges, or other irregularities.

In order to tackle this problem, a novel NDT method based on the features obtained instead from the PCA of frequency-domain impact-acoustics data is developed to enable a quantitative automatic inspection for defects assessment of tile-walls. The dynamics analysis of the impact process facilitates the theoretical interpretation of the acoustics characteristics in terms of the existence of bonding defects. The analytical result shows that in principle the energy distribution of the normalized PSD of impact sounds can serve as an indicator for defects detection.

However, in practice, the performance of traditional feature extraction, which directly employs the relative energies in different spectral zones as the feature vector, is seriously affected by the abnormal impact sounds caused by surface irregularities. Thus, this study presents a novel feature extraction method based on the PCA approach.

Clustering experiments carried out with the help of artificial sample slabs reveal that, while the existence of the surface non-uniformity seriously affects the separability of the feature vectors directly obtained from PSD, features extracted through PCA are more informative and useful than that based directly on frequency domain.

With the adoption of an ANN classifier and the alternative use of the 2-element feature vectors obtained from either the PCA or the original PSD features, the classification performance based on 200 signatures of each different type is thereafter presented and compared, demonstrating thereby the effectiveness of the presented PCA-based method. In view of the dimension reduction and clustering ability of PCA and with the use of neural network, the proposed NDE method, being low-cost, robust and convenient to use, offers the potential of being developed into a practical NDE scheme for automatic detection and characterization of bonding defects in tile-walls of high-rise buildings and similar bonding structures even with rough surfaces.

Acknowledgments

The authors are grateful for the funding of an RGC grant of the Hong Kong SAR (CityU 1166/02E) in support of the NATURAL project.

References

- [1] M.Y.L. Chew, Factors affecting ceramic tile adhesion for external cladding, *Construction and Building Materials* 13 (1999) 293–296.
- [2] K.S. Tan, K.C. Chan, B.S. Wong, L.W. Guan, Ultrasonic evaluation of cement adhesion in wall tiles, *Concrete Composites* 18 (1996) 119–124.
- [3] S. Yang, L. Gu, R.F. Gibson, Nondestructive of weak joints in adhesively bonded composite structures, *Composite Structures* 51 (2001) 63–71.
- [4] M. Sansalone, N.J. Carino, Detecting delaminations in concrete slabs with and without overlays using the impact-echo model, *ACI Materials Journal* 86 (2) (1989) 777–784.
- [5] M. Sansalone, W.B. Streett, *Impact-echo NDE of Concrete and Masonry*, Bullbrier Press, Ithaca, NY, 2003.
- [6] K. Mori, A. Spagnoli, A new non-contacting non-destructive testing method for defect detection in concrete, *NDT&E International* 35 (2002) 399–406.
- [7] T. Ito, T. Uomoto, Nondestructive testing method of concrete using impact acoustics, *NDT&E International* 30 (4) (1997) 217–222.
- [8] M. Asano, T. Kamada, M. Kunieda, K. Rokugo, Impact acoustics methods for defect evaluation in concrete, in: *Proceedings of Nondestructive Testing-Civil Engineering 2003 (NDT-CE2003)*, <http://www.ndt.net/article/ndtce03/papers/v040/v040.htm>
- [9] H. Wu, M. Siegel, Correlation of accelerometer and microphone data in the “Coin Tap Test”, in: *Proceedings of the Instrumentation and Measurement Technology Conference 99'*, Vol. 2, 1999, May 24–26, pp. 814–819.

- [10] M. Johnson, Waveform based clustering and classification of AE transients in composite laminates using principal component analysis, *NDT&E International* 35 (2002) 367–376.
- [11] C. Ding, X. He, *K*-means clustering via principle component analysis, in: *Proceedings of the 21st International Conference on Machine Learning*, Banff, Canada, 2004.
- [12] A. Sophian, G.Y. Tian, D. Taylor, J. Rudlin, A feature extraction technique based on principal component analysis for pulsed Eddy current NDT, *NDT&E International* 36 (2003) 37–41.
- [13] R.G. White, J.G. Walker, *Noise and Vibration*, Ellis Horwood Publishers, Chichester, UK, 1982.
- [14] S.P. Timoshenko, J.N. Goodier, *Theory of Elasticity*, McGraw-Hill, New York, 1970.
- [15] J.A. Zukas, T. Nicholas, H.F. Swift, L.B. Greszczuk, D.R. Curran, *Impact Dynamics*, Wiley, New York.
- [16] A.P. Christoforou, A.S. Yigit, Effect of flexibility on low velocity impact response, *Journal of Sound and Vibration* 217 (1998) 563–578.
- [17] C. Bonifazzi, E. Lodi, G. Maino, V. Muzzioli, L. Nanetti, N. Ludwig, M. Milazzo, A. Tartari, Investigation of defects in Fresco substrates by means of the ECoSP imaging system and the principal components image analysis, *Nuclear Instruments and Methods in Physics Research B* 213 (2004) 707–711.
- [18] Y. Xiang, S.K. Tso, Detection and classification of flaws in concrete structure using bispectra and neural networks, *NDT&E International* 35 (2003) 19–27.